

# Partial photoionization cross sections and angular distributions for double excitation of Helium up to the N=13 threshold

A. Czasch,<sup>1,\*</sup> M. Schöffler,<sup>1</sup> M. Hattaß,<sup>1</sup> S. Schößler,<sup>1</sup> T. Jahnke,<sup>1</sup> Th. Weber,<sup>1</sup> A. Staudte,<sup>1</sup> J. Titze,<sup>1</sup> C. Wimmer,<sup>1</sup> S. Kammer,<sup>1</sup> M. Weckenbrock,<sup>1</sup> S. Voss,<sup>1</sup> R. E. Grisenti,<sup>1</sup> O. Jagutzki,<sup>1</sup> L. Ph. Schmidt,<sup>1</sup> H. Schmidt-Böcking,<sup>1</sup> R. Dörner,<sup>1</sup> J.-M. Rost,<sup>2</sup> T. Schneider,<sup>2</sup> Chien-Nan Liu,<sup>3</sup> I. Bray,<sup>4</sup> A. S. Kheifets,<sup>5</sup> and K. Bartschat<sup>6</sup>

<sup>1</sup>Institut für Kernphysik, Universität Frankfurt, D-60486 Frankfurt, Germany

<sup>2</sup>Max-Planck-Institut für Physik komplexer Systeme, D-01187 Dresden, Germany

<sup>3</sup>Fu Jen Catholic University, Taipei, Taiwan

<sup>4</sup>Murdoch University, Perth, Western Australia 6150

<sup>5</sup>Australian National University, Canberra ACT 0200, Australia

<sup>6</sup>Drake University, Des Moines, Iowa 50311, USA

(Dated: to be submitted to Physical Review Letters)

Partial photoionization cross sections  $\sigma_N(E_\gamma)$  and photoelectron angular distributions  $\beta_N(E_\gamma)$  were measured for the final ionic states  $\text{He}^+(N > 4)$  in the region between the  $N=8$  and  $N=13$  thresholds ( $E_\gamma > 78.155$  eV) using the Coltrims technique. The experimental data are compared with two independent theoretical calculations. We find disagreement for the branching ratios to the various  $\text{He}_N^+$  states. Approaching the double ionization threshold the angular distributions indicate a simple mechanism (Wannier type) for the population of highly excited N states.

PACS numbers: 32.80.Dz, 32.80.Fb

In quantum theory Helium has always been considered as the archetypical counterpart of the classical three-body system. In 1963 Madden and Codling [1] investigated the double excitation of Helium into  ${}^1\text{P}^o$  states using synchrotron radiation. These measurements initiated a continuous sequence of theoretical [2–9] and experimental [10–14] work. Doubly-excited states become visible as resonances in the photon energy dependence of the single ionization cross section. These resonances are organized in series which converge towards the hydrogen-like final ionic  $\text{He}^+(N)$  states (also labeled as  $I_N$ ). The classification scheme which is most commonly used [2, 3] consists of five approximate quantum numbers  $N(K, T)_n^A$  which unambiguously denote doubly-excited states. Above  $I_{N=4}$  members of higher lying series interfere with lower series and act as so-called perturbers [9, 10]. Above  $I_{N=8}$  ( $E_\gamma > 78.155$  eV) the interaction between different series renders the identification of individual resonances impossible. In this regime the classification scheme  $N(K, T)_n^A$  is expected to break down giving rise to the question whether evidence for quantum chaos [15] manifested in Ericson fluctuations exists in Helium. Recently, theoretical calculations above  $I_{N=8}$  were analyzed using nearest neighbor spacing (NNS) statistics [14]. This analysis reveals a tendency towards a Wigner distribution which may be a first theoretical indication for quantum chaos.

Here we report the first measurement of continuous partial cross sections and angular distributions in this region in close vicinity to the double ionization threshold at 79.0052 eV. The partial cross sections show significant disagreement of up to a factor of two to theory. The measured angular distributions can be interpreted on the basis of a simple Wannier escape mechanism. This be-

havior was predicted by C. H. Greene [8] 25 years ago.

Historically the double excitation of Helium by photon absorption was investigated using a variety of different techniques. Originally [1] the total photon absorption cross section was measured as a function of the photon energy. However, during the last decades measurements of the total ionization yield were most common [10, 13] in which the overall  $\text{He}^+$  yield as a function of the photon energy is measured using gas cells. In a recent measurement [14] a photon energy of  $E_\gamma = 78.33$  eV was reached which is between the  $I_{N=8}$  and  $I_{N=9}$  threshold. Up to now this was the only available experimental data in the interesting regime close to the double ionization threshold at 79.0052 eV. A far more powerful technique for the investigation of autoionizing doubly excited states is electron spectroscopy. Measuring the kinetic energies of the emitted photo electrons allows for the separation of the final states  $N$  of the residual  $\text{He}^+(N)$  ions. The measured angular distribution of the emitted photo electrons is sensitive to the distribution of the contributing angular momenta  $\ell$ . As was shown in [12] the resonances of fairly weak series may reveal themselves as pronounced fluctuations of the angular distributions. The authors reported partial cross sections of photo electron emission  $\sigma_N(E_\gamma)$  and angular distributions  $\beta_N(E_\gamma)$  for  $\text{He}^+(N \leq 5)$ . In a more recent publication [11] partial cross sections were reported up to the threshold for  $\text{He}^+(N = 6)$  but no angular distributions were shown. With today's availability of computing power the interesting regime above  $N=8$  has become accessible for theorists [6, 7]. However, experimental research in this energy region remains an extremely demanding task due to very low partial cross sections. Both techniques - measurements of the total cross section on one side and electron spectroscopy on the other

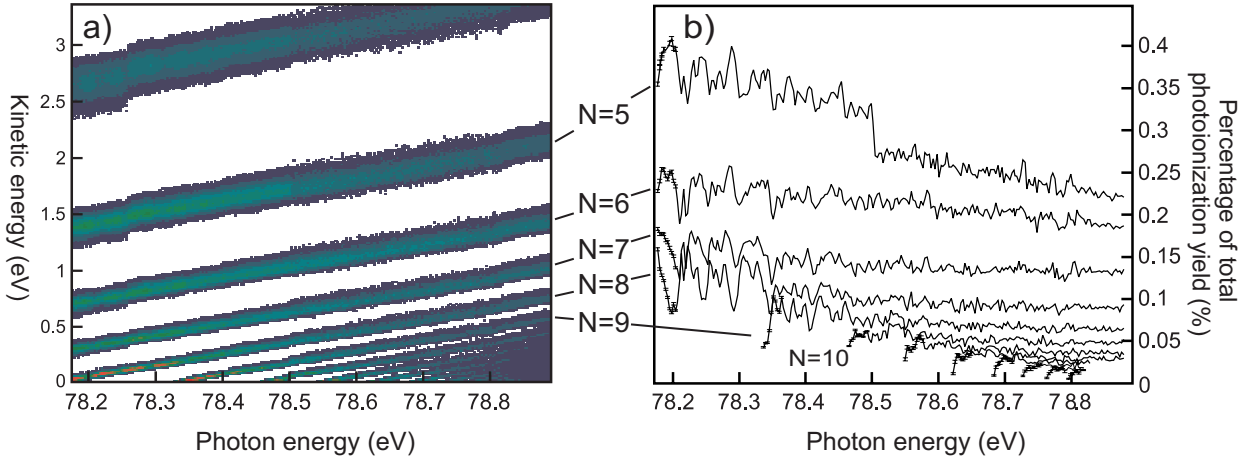


FIG. 1: In figure a the kinetic energies of the emitted photo electrons are displayed versus the photon energy. The lines can be assigned to different hydrogenlike final states  $N$  of the residual  $\text{He}^+(N)$  ions ( $N$  being the principal quantum number). Figure b contains the relative partial cross sections  $\sigma_N(E_\gamma)$ . The steplike structure in  $\sigma_{N=5}$  is an artefact of simple technical origin (the right part must be shifted upwards). The data was normalized by dividing the count rate of the various channels by the total number of detected  $\text{He}^+$  ions. This method ensures that fluctuations of the absolute count rate which might be caused by a non-constant target density or photon flux do not affect the results.

- suffer from this fact in different ways. Measuring total cross sections relies on the detection of small fluctuations in the presence of a huge background signal [10] which consists mostly of  $\text{He}^+(N = 1, 2)$  states. In contrast to this electron spectrometry seems to be well suited to solve these problems since it allows for the separation of different final states  $\text{He}^+(N)$ . However, the small angular acceptance of traditional electron spectrometers reduces the detection efficiency of these systems dramatically.

In order to overcome these obstacles we have applied the COLTRIMS imaging technique [16, 17] to the problem. Among the most striking advantages of these spectrometers is an angular acceptance of  $4\pi$  combined with multi-particle detection. Two time and position sensitive MCP-detectors [18] ( $\emptyset=80$  mm) combined with delay-line anodes for position readout are located vis-à-vis around the reaction zone. The photon beam intersects a narrow and cold supersonic Helium gas jet (density  $10^{12} \text{ cm}^{-2}$ ) which defines the geometry of the reaction zone. A weak homogenous electrostatic field (2 V/cm) guides the emitted particles towards the detectors. Thus electrons and  $\text{He}^+$  ions can be detected in coincidence. Since the fields inside the spectrometer are known quantities the reconstruction of the initial momenta is straight forward. The measurement was performed at the beamline U125/1-PGM at the German synchrotron facility BESSY II. At the beginning and at the end of the beamtime the degree of polarization (Stokes parameter  $S_1 = 1.0 \pm 1.8 \cdot 10^{-3}$ ) and the photon energy resolution of  $\Delta E_\gamma = 3.9 \text{ meV FWHM}$  were determined.  $\Delta E_\gamma$  was derived by scanning the  $2,1_4$  resonance at  $E_\gamma = 64.136 \text{ eV}$  and comparing the result with experimental and theoretical values in lit-

erature (e.g. [13]). The degree of linear polarization was determined by measuring the angular distribution of electrons emitted 0.5 eV above the single ionization threshold. The absolute energy calibration of the monochromator was achieved by locating the  $2,1_4$  resonance and the various thresholds for  $\text{He}^+(N > 8)$  using the simple formula  $E_N = 79.0052 \text{ eV} - 13.6 \text{ eV Z}^2 N^{-2}$ . The achieved absolute photon energy calibration is better than  $\pm 2.0 \text{ meV}$ . The acquired data set covers the photon energy region between  $E_\gamma = 78.155 \text{ eV}$  (threshold for  $\text{He}^+(N = 8)$ ) and  $E_\gamma = 78.88 \text{ eV}$ . For the scan a step size of 3 meV and a photon energy resolution of  $\Delta E_\gamma = 3.9 \text{ meV FWHM}$  was chosen. Between 78.48 eV and 78.792 eV the scan was performed with higher speed and less statistics per data point which causes larger error bars in this region. Final states up to  $N = 13$  could be clearly identified (fig. 1).

Figure 1a shows the kinetic energies of the emitted electrons in the photon energy range above  $E_\gamma > 78.155 \text{ eV}$ . The different lines can be assigned to the various final states of the residual  $\text{He}^+(N)$  ions. The intensity of these lines encodes the count rate of the corresponding autoionization channel. The intensities are shown in fig. 1b where the branching ratios (in %) between different reaction channels  $\text{He}^+(N)$  and the total cross section for  $\text{He}^+$  are displayed. The following discussion focuses on the region below 78.48 eV in which the scan was performed in a slower mode in order to determine data points with an appropriate statistical accuracy. The statistical error bars in this region are negligibly small. The most obvious feature is the similarity between different curves. Structures visible in curve  $N$  are also visible in curve  $N - 1$ . Additionally, there is a slight horizontal shift between

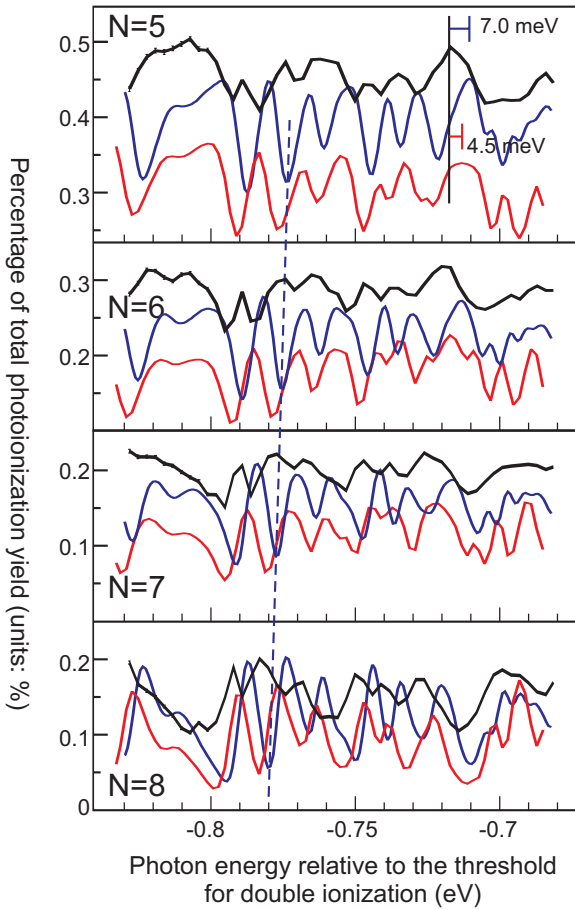


FIG. 2: Comparison between experiment (black) and theory. The blue (dark grey) curves correspond to R-matrix calculations [7] (velocity gauge) and the red (light grey) curves display CCC-calculations (velocity gauge). The statistical error bars indicated at the beginning of each black curve are very small. However there might be a systematical error (less than 10%) which might reduce the measured partial cross-sections as a whole. The theoretical data has been convoluted with a gaussian distribution of 3.9 meV FWHM. The photon energy scale is shown relative to the respective experimental or theoretical double ionization threshold (Exp 79.0052 eV, RM 79.006 eV, CCC 79.0089 eV).

different curves - in fig. 2 visualized as a tilted dashed line. This shift between  $N=5$  and  $N=8$  is about 7 meV. The reason for this behavior is unknown. However it is a feature that is well reproduced in both calculations. Since both calculations do not include relativistic effects nor the finite mass of the nucleus it is obvious that these factors can not be related to this behavior.

We compare the data to calculations [7] based on the eigenchannel R-Matrix method [21] using a close-coupling scheme [22] and to calculations applying the convergent close-coupling (CCC) approach [19]. The model of the latter is that the photon is absorbed by one of the He electrons, and then the problem becomes one of electron scattering on the  $\text{He}^+$  ion. More pre-

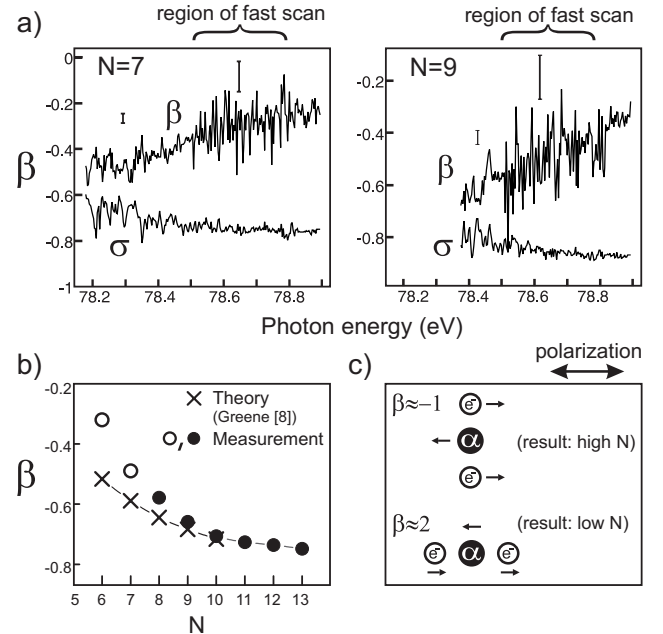


FIG. 3: a) The angular distributions ( $\beta$ -parameter) of photo electrons from different channels as a function of the photon energy. Additionally the partial cross sections  $\sigma_N$  are displayed in arbitrary units in order to demonstrate the correlation between both curves. Due to limitations in space the  $\beta$ -parameters for  $N = 5, 6, 8, 10$  are not shown. The larger error bars are assigned to the middle part of the scan where less statistics was acquired ( $78.48 \text{ eV} < E_\gamma < 78.792 \text{ eV}$ ). Theory can not yet reproduce the fluctuations of the  $\beta$ -parameters. b) Comparison with calculated  $\beta_N$  [8] at the beginning of each  $\beta_N$ -curve. The hollow circles (○) refer to data points which were not measured at the beginning of the corresponding curve and thus are shifted upwards due to the general (positive) slope of the  $\beta$ -curves. The errorbars are of the same size as the circles. c) This simple picture illustrates why highly excited final states are populated preferably in conjunction with  $\beta \approx -1$ .

cisely the final state of photoionization satisfies the same Schrödinger equation as for electron scattering on the  $\text{He}^+$  ion with a different asymptotic boundary condition. It is very important that a highly accurate description of the He ground state is used that produces essentially gauge-independent results [19]. In this case the cross sections for the three standard gauges V,A and L differ by less than 10 %. Recently, the original Laguerre-based CCC method was modified to allow the usage of a box-basis, which discretises the target spectrum by imposing the boundary condition that the eigenstates of the target Hamiltonian be zero at the box boundary  $R_0$  [20]. This approach is particularly attractive here because it readily allows the generation of large- $n$  eigenstates by simply increasing  $R_0$ . In the present case we took  $R_0 = 600 \text{ a.u.}$  which generated  $15-l$  negative-energy states of which  $13-l$  are good eigenstates. Here  $l \leq 5$  is the orbital angular momentum. We found that inclusion

of positive-energy states was also important. The total number of states taken for each  $l$  was  $22 - l$ , leading to a total of 117 states. The calculations were performed separately for each energy at a spacing of 2 meV. Thus resonances with a width of smaller than 2 meV might have been missed or might have been calculated with a too low intensity.

In fig. 2 the measured cross sections (branching ratios) are compared to both independent state-of-the-art calculations. The calculations are non-relativistic theories and do not account for the finite mass of the nucleus. These two effects in combination influence the absolute ground state energy (i.e. the double ionization threshold) by up to 10 meV. To account for these trivial effects and in order to compare all three data sets on one common energy scale we have plotted the curves relative to their respective threshold of double ionization. Almost all peaks and ditches found in the experiment are reproduced by both calculations. However the absolute position is shifted by up to 7 meV. Even more puzzling is the disagreement in the average values of the branching ratios. Surprisingly both theories disagree among each other by up to a factor of 1.5. Such disagreement between measurement and theory was also reported at lower photon energies  $E_\gamma < 76.8$  eV for  $N \leq 6$  [11]. Analog to our findings the measured cross sections in [11] were larger than predicted by theory. However, in an older experiment Menzel *et al.* [12] found good agreement between their experimental data and calculations for  $N \leq 4$ .

We now turn to the next level of detail. The  $\beta$ -parameter which characterizes the angular distribution shows similar rich structures as the partial cross sections (fig. 3a). From these complex patterns one might expect a breakdown of the  $N(K, T)_n^A$  scheme. However, this is misleading. Despite of all these overlapping resonances the underlying excitation and decay dynamics is very intuitive - it is even valid for the transition through the double ionization threshold. The onset values of  $\beta_N$  at their respective thresholds converge towards -1 as the double ionization threshold is approached from below. This was predicted by Greene [8] (based on Herricks SO(4) classification) and is in accordance with the situation just above threshold where Wannier law and experiment show a similar behavior [23]. In this picture the metastable  $e - \alpha - e$  configuration where the nucleus resides on the potential saddle between the two electrons plays a key role (fig. 3c). The preferred way how such a state can be populated is by absorption of a linear polarized photon. If the configuration is oriented perpendicular to the polarization vector the electric field of the photon can drive the system along the stable direction of the saddle. This means that the electrons have to be aligned perpendicular to the field vector (corresponding to  $\beta = -1$ ) and the nucleus is moved parallel to the polarization vector. Above the threshold for double ionization, this motion of the nucleus can be seen directly [23]. The other config-

uration, where the  $e - \alpha - e$  system is oriented parallel to the electric field results in the capture of one of the electrons in a more deeply bound state and hence does not contribute to high N states.

In conclusion the problem of double excitation of the most simple two electron system very close to the threshold for double ionization still poses a major challenge to theory and experiment. The angular distributions of near zero kinetic energy electrons indicate a simple excitation mechanism which is even valid for the transition through the threshold of double ionization and which can be understood in simple Wannier type stability considerations.

The experimental work was supported by the DFG and BMBF (Internationales Büro). We thank the German synchrotron facilities HASYLAB and BESSY II for financial support and beamtime. We are indebted to Dr. Reichardt, Dr. Follath and Dr. Möller for excellent support during the beamtimes. A.S. thanks the Studienstiftung des deutschen Volkes for support. A.C. and Th.W. thank Graduiertenförderung des Landes Hessen for support. I.B. and A.S.K acknowledge the support of the Australian Research Council. K.B. acknowledges the support of the National Science Foundation (USA).

- 
- \* Electronic address: czasch@atom.uni-frankfurt.de
- [1] R. P. Madden and K. Codling, Phys. Rev. Lett. **10**, 516 (1963).
  - [2] D. R. Herrick and O. Sinanoglu, Phys. Rev. A **11**, 97 (1975).
  - [3] C. D. Lin, Phys. Rev. Lett. **51**, 1348 (1983); Phys. Rev. A **29**, 1019 (1984).
  - [4] J. M. Feagin and J. S. Briggs, Phys. Rev. Lett. **57**, 984 (1986); Phys. Rev. A **37**, 4599 (1988).
  - [5] G. Tanner, K. Richter, and J.-M. Rost, Rev. Mod. Phys. **73**, 497 (2000).
  - [6] H. W. van der Hart and C. H. Greene, Phys. Rev. A **66**, 022710 (2002).
  - [7] T. Schneider, C.-N. Liu, and J.-M. Rost, Phys. Rev. A **65**, 042715 (2002).
  - [8] C. H. Greene, Phys. Rev. Lett. **44**, 869 (1980).
  - [9] J.-M. Rost, K. Schulz, M. Domke, and G. Kaindl, J. Phys. B **30**, 4663 (1997).
  - [10] M. Domke, K. Schulz, G. Remmers, and G. Kaindl, Phys. Rev. A **53**, 1424 (1996).
  - [11] Y. H. Jiang *et al.*, Phys. Rev. A **69**, 042706 (2004).
  - [12] A. Menzel *et al.*, Phys. Rev. Lett. **75**, 1479 (1995); Phys. Rev. A **54**, 2080 (1996).
  - [13] K. Schulz, G. Kaindl, and M. Domke, Phys. Rev. Lett. **77**, 3086 (1996).
  - [14] R. Püttner *et al.*, Phys. Rev. Lett. **86**, 3747 (2001).
  - [15] J.-P. Connerade, J. Phys. B **30**, L31 (1997).
  - [16] R. Dörner *et al.*, Phys. Rep. **330**, 96 (2000).
  - [17] J. Ullrich *et al.*, Rep. Prog. Phys. **66**, 1463 (2003).
  - [18] see <http://www.roentdek.com>
  - [19] A. Kheifets and I. Bray, Phys. Rev. A **57**, 2590 (1998).
  - [20] I. Bray, K. Bartschat, and A. T. Stelbovics, Phys. Rev. A **67**, 060704(R), (2003).

- [21] P. F. O'Mahony and C. H. Greene, Phys. Rev. A **31**, 250 (1985).
- [22] C. Pan, A. F. Starace, and C. H. Greene, Phys. Rev. A **53**, 840 (1996).
- [23] R. Dörner *et al.*, Phys. Rev. Lett. **77**, 1024 (1996).